

# RSC Advances



This is an *Accepted Manuscript*, which has been through the Royal Society of Chemistry peer review process and has been accepted for publication.

*Accepted Manuscripts* are published online shortly after acceptance, before technical editing, formatting and proof reading. Using this free service, authors can make their results available to the community, in citable form, before we publish the edited article. This *Accepted Manuscript* will be replaced by the edited, formatted and paginated article as soon as this is available.

You can find more information about *Accepted Manuscripts* in the [Information for Authors](#).

Please note that technical editing may introduce minor changes to the text and/or graphics, which may alter content. The journal's standard [Terms & Conditions](#) and the [Ethical guidelines](#) still apply. In no event shall the Royal Society of Chemistry be held responsible for any errors or omissions in this *Accepted Manuscript* or any consequences arising from the use of any information it contains.

# Modulating spin dynamics of Ln<sup>III</sup>-radical complexes by using different coligand

Ting Li,<sup>†</sup> Shang Yong Zhou,<sup>†</sup> Xin Li,<sup>†</sup> Li Tian,<sup>\*,†</sup> Dai Zheng Liao,<sup>‡</sup> Zhong Yi Liu,<sup>†</sup> and Jian Hua Guo

## Abstract

The combination of Ln<sup>III</sup> ion (Gd<sup>III</sup>, Tb<sup>III</sup> or Dy<sup>III</sup>) with a triazole nitronyl nitroxide radical results in six novel *2p-4f* compounds, namely, [Ln<sub>2</sub>(hfac)<sub>6</sub>(MeTrzNIT)(H<sub>2</sub>O)<sub>2</sub>]·1/2CH<sub>2</sub>Cl<sub>2</sub> (Ln = Gd(**1**), Tb(**2**), Dy(**3**); hfac = hexafluoroacetylacetone; MeTrzNIT = 2-{3-(5-methyl)-1,2,4-triazolyl}-4,4,5,5-tetramethylimidazoline-1-oxyl-3-oxide) and [Ln(Phtfac)<sub>3</sub>(MeTrzNIT)]<sub>2</sub>·C<sub>7</sub>H<sub>14</sub>·3H<sub>2</sub>O (Ln = Gd(**4**), Tb(**5**), Dy(**6**); Phtfac = 4,4,4-trifluoro-1-phenylbutane-1,3-dione). Single crystal X-ray diffraction studies revealed that compounds **1-3** are binuclear isostructural complexes, in which one MeTrzNIT molecular acts as a double-bridging ligand coordinated to two Ln<sup>III</sup> ions through its two NO groups and two nitrogen atoms of the triazole ring. In **1-3**, the coordination number around the lanthanide ion is nine, and the polyhedron is a 4,4,4-tricapped trigonal prism (*D*<sub>3h</sub>). While the larger steric hindrance of Ph- group than CF<sub>3</sub>- in Phtfac ligand induces complexes **4-6** to be mononuclear bi-spin compounds, in which central Ln<sup>III</sup> ions are coordinated by three Phtfac and one bidentate MeTrzNIT radical. The coordination number around the lanthanide ion in **4-6** is eight, and the polyhedron is in a square antiprism geometry (*D*<sub>4d</sub>). Compounds **3** and **5** was found to exhibit slow relaxation of the magnetization, suggesting single-molecule magnet (SMM)

<sup>†</sup>Tianjin Key Laboratory of Structure and Performance for Functional Molecules, Key Laboratory of Inorganic-Organic Hybrid Functional Materials Chemistry (Tianjin Normal University), Ministry of Education, , Tianjin 300387, P. R. China. E-mail: [lilytianli@hotmail.com](mailto:lilytianli@hotmail.com)

<sup>‡</sup>Department of Chemistry and Key Laboratory of Advanced Energy Materials Chemistry (MOE), Nankai University, Tianjin 300071, P. R. China.

behavior, while no ac signal is noticed for compounds **2** and **6**. The different magnetic relaxation behaviours between **2** and **5**, or between **3** and **6**, are due to the different crystal structure around the Ln<sup>III</sup> ions and the magnetic interaction. It is demonstrated that the  $\beta$ -diketonate coligand may play an important role in determining the spin dynamic for the lanthanide-radical system.

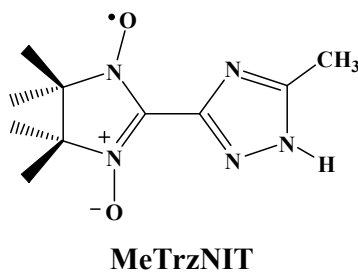
**Keywords:** Triazole nitronyl nitroxide radical, Lanthanide complexes, Magnetic property, Single-molecule magnet

## Introduction

Designing and synthesizing of low-dimensional assemblies based on anisotropic metal ions that show magnetization relaxation have attracted much attention.<sup>1,2</sup> Such materials named as single-molecular magnets (SMMs) and single chain magnets (SCMs), have the potential applications in high-density data storage, quantum information processing systems, and spintronic devices.<sup>3-5</sup> The general character of SMMs is that the magnetic bistability arises from the blocking anisotropy without long-range ordering. One of the challenging problems in this field is to increase blocking temperature at which superparamagnetic behavior can occur, which depends on the anisotropy barrier from a combination of the appropriate spin in the ground state and uniaxial magnetic anisotropy.<sup>6</sup> Lanthanides ions, especially heavy lanthanide ions, have large number of unpaired *f*-electrons and large intrinsic magnetic anisotropy, and have become good candidates for the construction of SCMs and SMMs.<sup>7-10</sup> But, the naturally accompanying quantum tunneling from the hyperfine couplings and dipolar spin-spin interactions of lanthanide ions always lowers the effective relaxation energy barrier and induces the loss of remnant magnetization.<sup>11</sup> Recent studies show that strong coupling through a radical bridge (with a record blocking temperature) and strong axially or Ising exchange interaction can suppress quantum tunneling to provide strategies for enhancing the SMM properties.<sup>12</sup> Nitronyl nitroxide radicals (NITs) as spin carriers are fascinating building blocks and bridges not only for their stabilization under ambient condition but also for the  $\pi$  systems to transfer the effective magnetic

interactions. The use of organic radicals has been proved to be an attractive route to obtain magnetically coupled 4*f*-organic radical heterospin systems.<sup>13,14</sup>

For SMMs containing lanthanide ion, magnetic relaxation is very sensitive to the symmetry of the ligand field of the rare earth ion and the spin dynamic can be modified by the careful adjustment of the ligand field around the metal center. In order to explore how the symmetry of the local crystal field around the lanthanide center affect the spin dynamics of the complex, we decided to use two  $\beta$ -diketonate coligands hexafluoroacetylacetonate (hfac) and 4,4,4-trifluoro-1-phenylbutane-1,3-dione (Phtfac) to construct radical-lanthanide SMMs. The introduction of a Ph- group in the  $\beta$ -diketonate ligand may modify the ligand field of the metal ion, thus adjusting the magnetic relaxation of the molecule. Herein we synthesized six lanthanide compounds based on a triazole nitronyl nitroxide radical (MeTrzNIT = 2-{3-(5-methyl)-1,2,4-triazolyl}-4,4,5,5-tetramethylimidazoline-1-oxyl-3-oxide) and coligand hfac or Phtfac, namely,  $[\text{Ln}_2(\text{hfac})_6(\text{MeTrzNIT})(\text{H}_2\text{O})_2] \cdot 1/2\text{CH}_2\text{Cl}_2$  (Ln = Gd(**1**), Tb(**2**), Dy(**3**)) and  $[\text{Ln}(\text{Phtfac})_3(\text{MeTrzNIT})]_2 \cdot \text{C}_7\text{H}_{14} \cdot 3\text{H}_2\text{O}$  (Ln = Gd(**4**), Tb(**5**), Dy(**6**)). Magnetic studies showed that complexes **3** and **5** exhibit frequency-dependent ac susceptibility at low temperature, which suggest SMMs behavior. The comparison of the magnetic properties of **2** and **5** or **3** and **6** highlights that the  $\beta$ -diketonate ligands can play an important role in modulating the magnetic relaxation.



**Scheme 1.** Structure of the triazole nitronyl nitroxide radical ligand.

## Experimental Details

### Materials and physical measurements

All of the reagents used in the syntheses were of analytical grade, except that the solvents used were dried (heptane over sodium, CH<sub>2</sub>Cl<sub>2</sub> over CaH<sub>2</sub> and CHCl<sub>3</sub> over P<sub>2</sub>O<sub>5</sub>) and distilled prior to use. The starting materials Ln(hfac)<sub>3</sub>·2H<sub>2</sub>O and Ln(Phtfac)<sub>3</sub>·2H<sub>2</sub>O were synthesized according to methods in the literature.<sup>15</sup> MeTrzNIT = 2-{3-(5-methyl)-1,2,4-triazolyl}-4,4,5,5-tetramethylimidazoline-1-oxyl-3-oxide) was prepared based on the literature method.<sup>16</sup> Elemental analyses for carbon, hydrogen, and nitrogen were performed on a Perkin–Elmer 240 elemental analyzer. Infrared spectra were recorded from KBr pellets in the 4000–400 cm<sup>-1</sup> region on a Bruker TENOR 27 spectrometer. Powder X-ray diffraction measurements were recorded on a D/Max-2500 X-ray diffractometer using Cu-Kα radiation. Direct-current (dc) magnetic susceptibilities of crystalline samples were measured on an MPMS-7 SQUID magnetometer in the temperature range of 2–300 K with 1000 Oe applied magnetic field. Alternating-current (ac) susceptibilities were performed on the same magnetometer under zero static field with an oscillating of 3.5 Oe at frequencies up to 1500 Hz. The data were corrected for the diamagnetism of the samples using Pascal constants.

### Preparation of complexes of 1–6

Complexes **1–3** were obtained by dissolving Ln(hfac)<sub>3</sub>·2H<sub>2</sub>O (0.1 mmol) (Ln = Gd (**1**), Tb (**2**), Dy (**3**),) in boiling *n*-heptane (20 mL). After stirring for 2 h, the solution was cooled to 60 °C, to which MeTrzNIT (0.05 mmol) in CH<sub>2</sub>Cl<sub>2</sub> (5 mL) was added. The mixture was refluxed for 30 min. Then the solution was cooled to room temperature, filtrated and the filtrate was stored in a refrigerator at 0–4 °C for three or four weeks to give blue-violet crystals, which were suitable for X-ray analysis.

Complexes **4–6** were obtained by dissolving Ln(Phtfac)<sub>3</sub>·2H<sub>2</sub>O (0.1 mmol) (Ln = Gd(**4**), Tb (**5**), Dy (**6**),) in boiling *n*-heptane (30 mL). After stirring for 2 h, the solution was cooled to 60 °C, to which MeTrzNIT (0.1 mmol) in CH<sub>2</sub>Cl<sub>2</sub> (5 mL) was added. The mixture was refluxed for 30 min. Then the solution was cooled to room temperature, filtrated and the filtrate was stored in a refrigerator at 0–4 °C for four or five weeks to give blue-violet crystals.

[Gd<sub>2</sub>(hfac)<sub>6</sub>(MeTrzNIT)(H<sub>2</sub>O)<sub>2</sub>]<sub>2</sub>·1/2CH<sub>2</sub>Cl<sub>2</sub> (**1**): Yield 0.068 g, 72%.

$C_{40.5}H_{27}ClF_{36}Gd_2N_5O_{16}$  (1873.62): calcd. C 25.96, H 1.45, N 3.74; found: C 25.54, H 1.32, N 3.55%. IR (KBr pellet,): 2354 (w), 1662 (w), 1383 (m), 1150 (s), 1078 (vs), 960 (m), 863 (vs), 544 (vs)  $cm^{-1}$ .

**[Tb<sub>2</sub>(hfac)<sub>6</sub>(MeTrzNIT)(H<sub>2</sub>O)<sub>2</sub>].1/2CH<sub>2</sub>Cl<sub>2</sub> (2):** Yield 0.064 g, 68%.  $C_{40.5}H_{27}Tb_2ClF_{36}N_5O_{16}$  (1876.96): calcd. for C 25.91, H 1.45, N 3.73; found: C 25.82, H 1.52, N 3.52%. IR (KBr pellet): 2352 (w), 1655 (w), 1386 (m), 1148 (vs), 1079 (vs), 973 (m), 848 (s), 538 (s)  $cm^{-1}$ .

**[Dy<sub>2</sub>(hfac)<sub>6</sub>(MeTrzNIT)(H<sub>2</sub>O)<sub>2</sub>].1/2CH<sub>2</sub>Cl<sub>2</sub> (3):** Yield 0.059 g, 64%.  $C_{40.5}H_{27}ClDy_2F_{36}N_5O_{16}$  (1884.13): calcd. C 25.82, H 1.44, N 3.72; found: C 26.12, H 1.27, N 3.78%. IR (KBr pellet,): 1663 (w), 1395 (w), 1153 (s), 1081 (vs), 952 (m), 859 (m), 553 (s)  $cm^{-1}$ .

**[Gd(Phtfac)<sub>3</sub>(MeTrzNIT)]<sub>2</sub>.C<sub>7</sub>H<sub>14</sub>.3H<sub>2</sub>O (4):** Yield 0.071 g, 63%.  $C_{87}H_{90}F_{18}Gd_2N_{10}O_{19}$  (2236.18): calcd. C 46.73, H 4.06, N 6.27; found: C 46.52, H 3.68, N 6.04%. IR (KBr pellet,): 3151(vs), 1617 (s), 1578 (w), 1531 (w), 1459 (w), 1402 (s), 1290 (m), 1190 (s), 1139 (s), 776 (m), 704 (m), 631 (s)  $cm^{-1}$ .

**[Tb(Phtfac)<sub>3</sub>(MeTrzNIT)]<sub>2</sub>.C<sub>7</sub>H<sub>14</sub>.3H<sub>2</sub>O (5):** Yield 0.078 g, 69%.  $C_{87}H_{90}F_{18}Tb_2N_{10}O_{19}$  (2240.5): calcd. C 46.64, H 4.05, N 6.25; found: C 46.41, H 3.81, N 6.13%. IR (KBr pellet,): 3164(vs), 1616 (s), 1572 (w), 1538 (w), 1469 (w), 1401 (s), 1291 (m), 1190 (s), 1140 (s), 762 (m), 703 (m), 626 (s)  $cm^{-1}$ .

**[Dy(Phtfac)<sub>3</sub>(MeTrzNIT)]<sub>2</sub>.C<sub>7</sub>H<sub>14</sub>.3H<sub>2</sub>O (6):** Yield 0.072 g, 64%.  $C_{87}H_{90}F_{18}Dy_2N_{10}O_{19}$  (2246.61): calcd. C 46.50, H 4.04, N 6.24; found: C 46.16, H 3.75, N 6.31%. IR (KBr pellet,): 3156(vs), 1617 (s), 1578 (w), 1531 (w), 1467 (w), 1402 (s), 1291 (m), 1186 (s), 1139 (s), 762 (m), 698 (m), 631 (s)  $cm^{-1}$ .

### X-Ray crystallography

The crystallographic data of compounds **1-4** were carried out with an Oxford Diffractometer SuperNova TM, which were equipped with graphite monochromatic Mo-K $\alpha$  radiation ( $\lambda = 0.71073 \text{ \AA}$ ). Lorentz polarization and absorption corrections were applied. Structures were solved by direct methods with the SHELXS-97 program and

refined by full-matrix least-squares techniques against  $F^2$  with the SHELXTL-97 program package.<sup>17</sup> Some restraints are applied, such as ISOR (anisotropic parameter), DFIX (restricting the distance between two atoms) to solve the disorder of the F atoms and  $\text{CH}_2\text{Cl}_2$  in **2** and **3**. Besides fluorine atoms, all other non-hydrogen atoms were refined anisotropically, and hydrogen atoms were located and refined isotropically. Although complex **4** successfully underwent X-ray analysis after many times' experiments, it couldn't give good crystallography data because the crystals are easy to efflorescence. The  $R_1$  and  $wR_2$  data of **4** are a little larger than the normal data. For complexes **5** and **6**, the crystals are much easier to be weathered than **4** and they can't undergo X-ray analysis even at low temperature. Powder X-ray diffraction, elemental analysis, and infrared spectroscopy confirmed that complexes **5** and **6** are isomorphous to **4**. Crystallographic data for the compounds **1-4** are listed in Table 1 and the powder X-ray diffraction data for all the six compounds are shown in the Supporting Information Section (Fig. S1-2)

## Results and discussion

### Crystal structure

**Structure of 3.** Single-crystal X-ray diffraction analyses reveal that complexes **1-3** are isomorphous and belong to monoclinic  $C2/c$  space group with  $Z = 8$ . In view of their structural similarity, only the structure of **3** will be described herein as a representative example. The structural diagrams of **1-2** are given in the Supporting Information, Fig. S3-S4. As shown in Fig. 1, two  $\text{Dy}(\text{hfac})_3$  units are connected by a radical ligand MeTrzNIT to give a binuclear core. The center ions are all surrounded with a slightly distorted 4,4,4-tricapped trigonal prism ( $D_{3h}$ )  $\text{DyO}_8\text{N}$  coordination sphere from three bischelate hfac anions and one bridging radical ligand. The Dy–O(N) (nitroxide) distances are 2.408(6) and 2.416(5) Å, respectively. The Dy–O(hfac) bond lengths are in the range of 2.337(6)–2.478(5) Å, the Dy–N3 and Dy–N5 distances are longer than the normal Dy–N bonds ascribed to the bridged character of N3 and N5 (Table S1). Each MeTrzNIT acts as a double-bridging ligand and is coordinated to two different

Dy<sup>III</sup> ions through the two oxygen atoms of NO groups and two nitrogen atoms of the triazole ring. The Dy<sup>III</sup>···Dy<sup>III</sup> separation distance in every binuclear unit is 7.277(5) Å and the shortest intermolecular Dy<sup>III</sup>···Dy<sup>III</sup> separation is 5.995(6) Å. Here the five membered imidazoline ring and the triazole ring show average twist angles of 16.6(2)°. The five-membered ring of the radical deviates significantly from planarity with C20 atom 0.045 Å above the average plane.

**Table 1.**  
Crystallographic Data and Structure Refinement Details for **1–4**.

	<b>1</b>	<b>2</b>	<b>3</b>	<b>4</b>
formula	C <sub>40.5</sub> H <sub>27</sub> ClF <sub>36</sub> Gd <sub>2</sub> N <sub>5</sub> O <sub>16</sub>	C <sub>40.5</sub> H <sub>27</sub> Tb <sub>2</sub> ClF <sub>36</sub> N <sub>5</sub> O <sub>16</sub>	C <sub>40.5</sub> H <sub>27</sub> ClDy <sub>2</sub> F <sub>36</sub> N <sub>5</sub> O <sub>16</sub>	C <sub>87</sub> H <sub>90</sub> F <sub>18</sub> Gd <sub>2</sub> N <sub>10</sub> O <sub>19</sub>
Mr	1873.62	1876.96	1884.13	2236.15
crystal system	monoclinic	monoclinic	monoclinic	monoclinic
space group	<i>C2/c</i>	<i>C2/c</i>	<i>C2/c</i>	<i>C2/c</i>
<i>a</i> (Å)	25.752(4)	25.7993(9)	25.805(5)	27.474(2)
<i>b</i> (Å)	24.466(4)	24.4562(9)	24.464(5)	21.7415(18)
<i>c</i> (Å)	23.085(3)	23.1575(9)	23.177(5)	33.465(3)
$\alpha$ (°)	90	89.34(3)	90	90
$\beta$ (°)	120.758(4)	120.85(2)	120.81(3)	102.2500(10)
$\gamma$ (°)	90	90	90	90
<i>V</i> (Å <sup>3</sup> )	12499(3)	12544.6(8)	12567(4)	19535(3)
<i>Z</i>	8	8	8	8
$\rho$ calc (Mg/m <sup>3</sup> )	1.991	1.988	1.947	1.414
$\mu$ (mm <sup>-1</sup> )	2.319	2.451	2.530	1.442
<i>F</i> (000)	7216	7232	7080	8272
$\theta$ range (°)	1.66–25.01	1.84–25.01	1.24–25.01	1.245–28.379
GOF on <i>F</i> <sup>2</sup>	1.043	1.030	1.069	1.075
<i>R</i> <sub>1</sub> , <i>wR</i> <sub>2</sub> [ <i>I</i> > 2 $\sigma$ ( <i>I</i> )]	0.0508, 0.1208	0.0383, 0.0766	0.0583, 0.1424	0.1082, 0.2385
<i>R</i> <sub>1</sub> , <i>wR</i> <sub>2</sub> (all data)	0.0707, 0.1373	0.0518, 0.0834	0.0714, 0.1498	0.2163, 0.2911

**Structure of 4.** Compound **4** also crystallizes in space group *C2/c* with *Z* = 8. The asymmetric unit contains two crystallographically independent [Gd(Phtfac)<sub>3</sub>(MeTrzNIT)] moieties, and every [Gd(Phtfac)<sub>3</sub>(MeTrzNIT)] exhibits mononuclear structure with central metal ion in an LnO<sub>7</sub>N coordination sphere (Fig 2). Powder X-ray diffraction, confirmed that complexes **5** and **6** are isomorphous to **4**. As shown in Fig. 2a, each central Gd<sup>III</sup> ion is eight-coordinated with three bidentate  $\beta$ -diketonate coligands and one bidentate MeTrzNIT radical ligand. The Gd–O(Phtfac) distances range from 2.313(8) to 2.392(9) Å. The Gd–O(radical) and Gd–N(triazole)

bond lengths of compound **4** are in the range of 2.365(8)–2.386(8) Å and 2.653(8)–2.697(8) Å, respectively. When applying the  $D_{4d}$  symmetry to the  $GdO_8$  site, CSM method gives the Gd1 and Gd2 the minimal value of  $S = 0.434$  or  $S = 0.621$ , respectively.

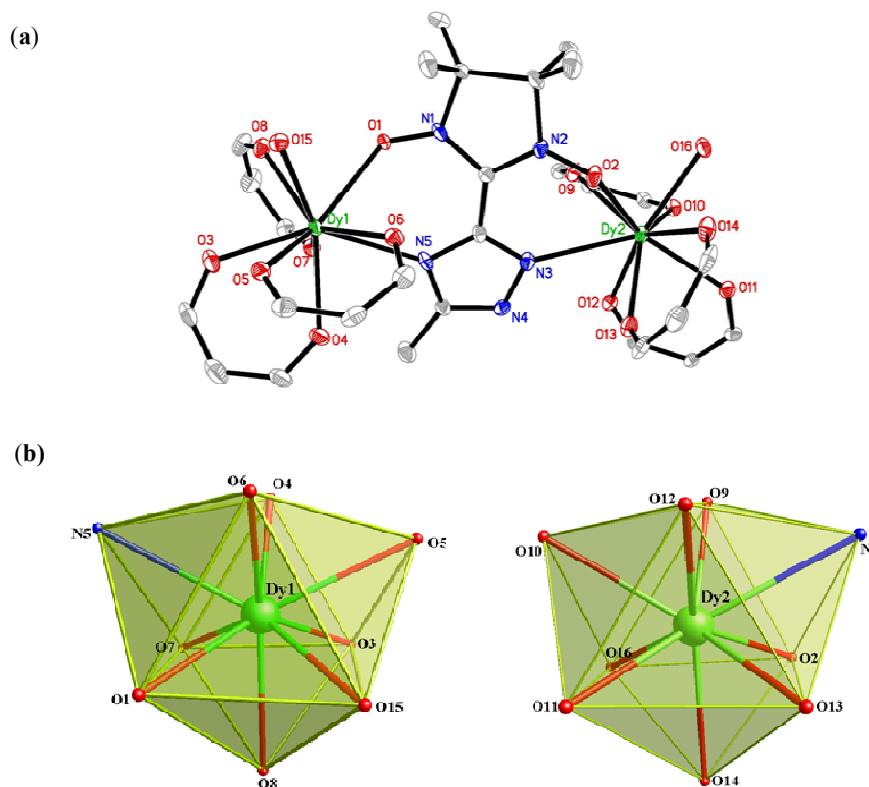


**Fig. 1.** (a) Simplified view of the crystal structure of **3**. Fluorine, hydrogen, and some carbon atoms are omitted for clarity. (b) Polyhedral representation of the  $Dy^{3+}$  cores.

## Magnetic Properties

**Static Magnetic Properties for 1-3.** Variable temperature magnetic susceptibilities for complexes **1-3** are studied and shown in Fig. 3. At room temperature, the  $\chi_M T$  value is 16.53  $\text{cm}^3 \cdot \text{K} \cdot \text{mol}^{-1}$  for complex **1**, which is close to the expected values of 16.29  $\text{cm}^3 \cdot \text{K} \cdot \text{mol}^{-1}$  for the isolated spins of two  $Gd^{III}$  ions ( $^8S_{7/2}$ ,  $g = 2$ ) and one radical ( $S = 1/2$ , 0.375  $\text{cm}^3 \cdot \text{K} \cdot \text{mol}^{-1}$ ). On decreasing the temperature, the  $\chi_M T$  value almost remains unchanged till 50 K. Then it begins to increase quickly as the temperature is lowered

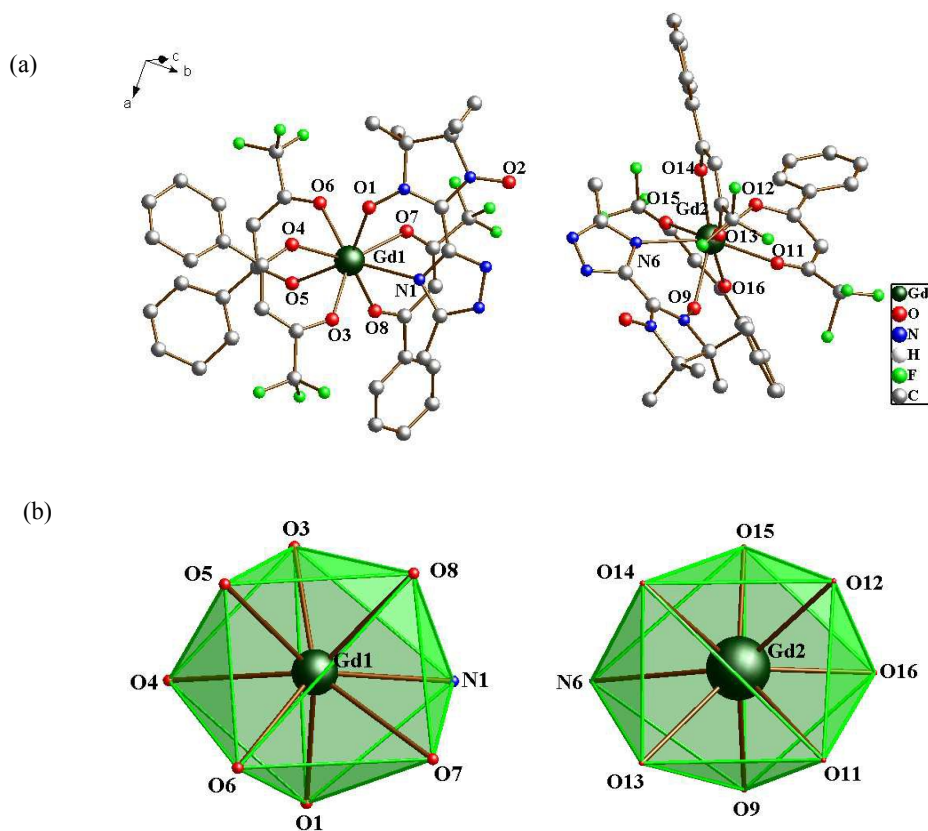


**Fig. 2.** (a) Simplified view of the crystal structure of **5**. Fluorine, hydrogen, and some carbon atoms are omitted for clarity. (b)  $D_{4d}$ -symmetry polyhedral of gadolinium atoms.

further and reaches a peak value of  $19.14 \text{ cm}^3 \cdot \text{K} \cdot \text{mol}^{-1}$  at 2 K. The profile of the curve indicates that the  $\text{Gd}^{\text{III}}$  ion and nitroxide radical interactions are ferromagnetic. Based on the above structural analysis, two main exchange pathways should be operative: (i) the magnetic interaction between Gd and the directly coordinated nitroxide group ( $J$ ); (ii) the magnetic coupling between Gd(1) and Gd(2) through triazole ring ( $J'$ ). Accordingly, the system was modeled as a tri-spin unit, and the magnetic analysis for  $\text{Gd}^{\text{III}}$ -Rad unit was carried out by using the spin Hamiltonian  $\hat{H} = -2J(\hat{S}_{\text{Gd1}}\hat{S}_{\text{rad1}} + \hat{S}_{\text{Gd2}}\hat{S}_{\text{rad1}}) - 2J'\hat{S}_{\text{Gd1}}\hat{S}_{\text{Gd2}}$ . Equation S1-S2 (which is shown in Supporting Information Section) is introduced to analyze the magnetic coupling strength, where  $J$  and  $J'$  represent the magnetic coupling for Gd-radical and Gd1-Gd2, respectively. The weak exchange interaction being considered within the mean field approximation ( $zj'$ ).<sup>18</sup>

The observed  $\chi_M T$  data were well reproduced, giving the best fitting parameters of  $g_{\text{Gd}} = 1.99$ ,  $J = 1.65 \text{ cm}^{-1}$ , and  $J' = -0.1724 \text{ cm}^{-1}$ ,  $zj' = 0.0043 \text{ cm}^{-1}$  with  $R = 1.38 \times 10^{-3}$  ( $g_{\text{R}}$  and  $g$  was fixed as 2). The positive values of  $J$  indicate the ferromagnetic interactions between  $\text{Gd}^{\text{III}}$  ion and the radical, which is very common in Gd–radical complexes.<sup>19</sup> The antiferromagnetic reaction  $J'$  between the two  $\text{Gd}^{\text{III}}$  ions through imidazoline and triazole rings is quite weak.<sup>20-21</sup> The magnetization *versus* field measurements at 2 K is shown in Fig. 4 (left). A magnetization of  $15.08 N\beta$  is reached at 50 kOe, in agreement with the  $14.96 N\beta$  for the ferromagnetic arrangement for the spins.

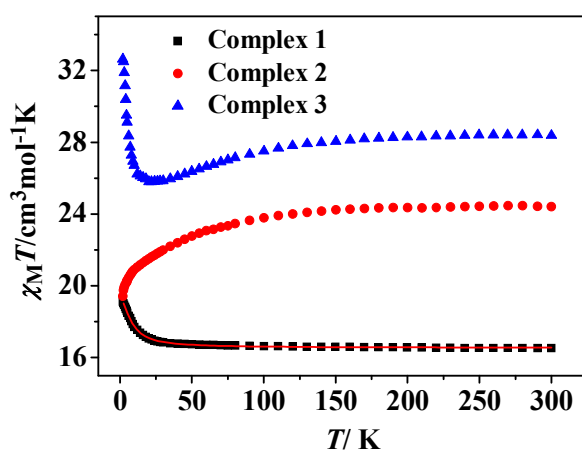


**Fig. 3.** Temperature dependence of  $\chi_M T$  values for complexes **1-3**. The solid line represents the theoretical values based on the corresponding equations.

For **2** (Fig. 3), the value of  $\chi_M T$  at 300 K is  $24.41 \text{ cm}^3 \cdot \text{K} \cdot \text{mol}^{-1}$ , which is a little higher than the expected value  $23.84 \text{ cm}^3 \cdot \text{K} \cdot \text{mol}^{-1}$  for two uncoupled  $\text{Tb}^{\text{III}}$  ions ( ${}^7\text{F}_6$  and  $g = 3/2$ ) and one organic radical ( $S = 1/2$ ). At high temperature (130–300 K), the value of  $\chi_M T$  almost remains unchanged. As the temperature is lowered from 130 K,  $\chi_M T$  decreases to reach  $19.43 \text{ cm}^3 \cdot \text{K} \cdot \text{mol}^{-1}$  at 2 K. The decrease of the  $\chi_M T$  values in the high temperature regime is most probably governed by the depopulation of the  $\text{Tb}^{\text{III}}$  Stark sublevels. The decrease of  $\chi_M T$  at low temperature suggests the presence of intramolecular antiferromagnetic interaction. This magnetic behavior may be ascribed to the exchange

interaction between the paramagnetic ions (Rad-Tb(III), Tb(III)-Tb(III) interaction through triazole ring) combined with the crystal field and spin-orbit effect. At present, it is not possible to quantify the different contributions,<sup>22</sup> but the crystal field and spin-orbit effect may be dominant due to the completed 5s and 5p subshells shielding 4f electrons.<sup>23</sup> The field dependences of magnetization ( $M$ ) for complex **2** have been determined at 2 K in the range of 0–70 kOe (Fig. 4 (right)). The field-dependent magnetization values below 10 K show a rapid increase in the magnetization at low magnetic fields. The maximum magnetization is  $11.8 N\beta$  at 2 K and 70 kOe, which does not reach the expected saturation values of  $19 N\beta$  ( $18 N\beta$  for two Tb<sup>III</sup> ions for  $J = 6$  and  $g = 3/2$ , plus  $1 N\beta$  for an organic radical), most likely because of the crystal field effect on the Tb<sup>III</sup> ion.<sup>24</sup>

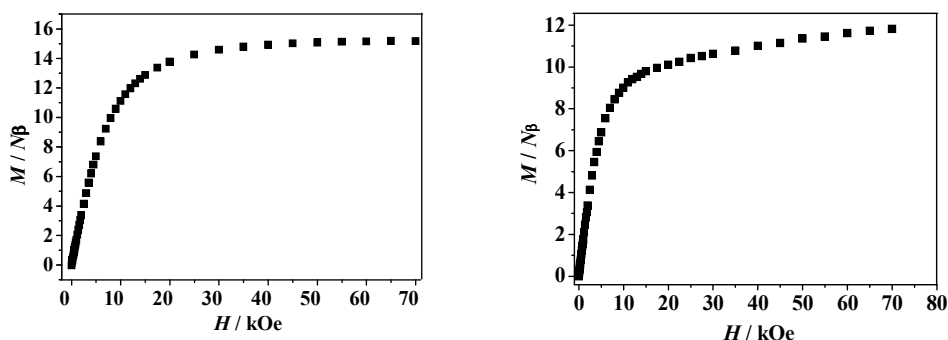


**Fig. 4.** Field dependence of the magnetization at 2 K for complex **1**(left) and **2**(right).

For **3**, the value of  $\chi_M T$  at room temperature is  $28.38 \text{ cm}^3 \cdot \text{K} \cdot \text{mol}^{-1}$ , which is slightly lower than the expected value of  $28.70 \text{ cm}^3 \cdot \text{K} \cdot \text{mol}^{-1}$  for two isolated Dy<sup>III</sup> ions ( ${}^6\text{H}_{15/2}$ ) and one organic radical ( $S = 1/2$ ). As the temperature is lowered,  $\chi_M T$  decreases slowly to reach a minimum of  $25.97 \text{ cm}^3 \cdot \text{K} \cdot \text{mol}^{-1}$  at 20 K. Below 20 K,  $\chi_M T$  increases dramatically to reach a peak value of  $32.63 \text{ cm}^3 \cdot \text{K} \cdot \text{mol}^{-1}$  at 2 K. The decrease of  $\chi_M T$  upon lowering of the temperature in the high-temperature range is most probably governed by depopulation of the Ln<sup>III</sup> Stark sublevels. The marked increase of  $\chi_M T$  at low temperature indicates the presence of ferromagnetic interactions. The field dependences of magnetization ( $M$ ) for complex **3** have been determined at 2–5 K in the

range of 0-70 kOe (Fig. 5a). The field-dependent magnetization value below 5 K shows a rapid increase at low magnetic fields. At higher fields,  $M$  increases up to  $12.79 N\beta$  at 2 K and 70 kOe, which does not reach the expected saturation values of  $21 N\beta$  ( $10 N\beta$  for each  $\text{Dy}^{\text{III}}$  ion for  $J = 15/2$  and  $g = 4/3$ , plus  $1 N\beta$  for the organic radical). The nonsuperposition on the  $M$  versus  $H/T$  curves at different temperatures indicates the presence of a magnetic anisotropy and/or low lying excited states in the system, which corresponds to the reported results.<sup>8b,9a,23,24,25,26</sup> Fig. 5b shows the magnetization versus field curve at the temperature of 2 K, but no hysteresis loop was observed.

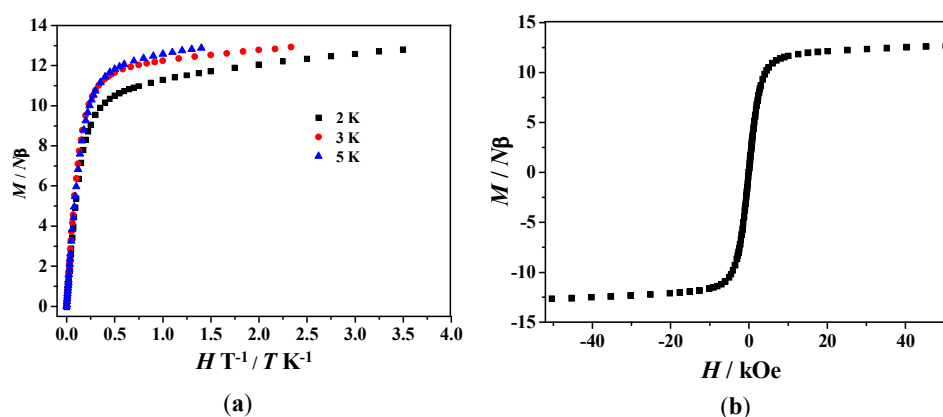


**Fig. 5.** (a) Field dependence of the magnetization at different temperatures for complex 3. (b) Magnetization versus field measurement for complex 3 as a polycrystalline sample at 2 K.

**Static Magnetic Properties for 4-6.** The temperature dependence of magnetic susceptibilities for 4-6 in the 2–300 K range is studied and shown in Fig. 6. For complex 4, the observed room temperature  $\chi_M T$  value is  $8.62 \text{ cm}^3 \cdot \text{K} \cdot \text{mol}^{-1}$ , in agreement with the expected value  $8.44 \text{ cm}^3 \cdot \text{K} \cdot \text{mol}^{-1}$  for one uncoupled  $\text{Gd}^{\text{III}}$  ion ( $^8S_{7/2}$ ,  $g = 2$ ) and one organic radicals ( $S = 1/2$ ). On decreasing the temperature, the  $\chi_M T$  value steadily increases and begins to increase more sharply at 30 K till to reach a peak value of  $9.72 \text{ cm}^3 \cdot \text{K} \cdot \text{mol}^{-1}$  at 2 K. The overall magnetic behavior indicates ferromagnetic interactions between the  $\text{Gd}^{\text{III}}$  ion and nitroxide radicals. Accordingly, the system was modeled as a mononuclear bi-spin unit, and the magnetic analysis was carried out by

using the spin Hamiltonian  $H = -2J_{\text{Rad-Gd}}\hat{S}_{\text{Rad}}\hat{S}_{\text{Gd}}$ , where  $J_{\text{Rad-Gd}}$  characterized the exchange interactions for radical-Gd(III). Assuming that the radical and Gd(III) have the same  $g$  value, the magnetic data were analyzed by the following approximate treatment eqn. (1-2). The mean-field approximation ( $zj'$ ) was introduced to indicate the possible interactions between mononuclear moleculars.

$$\chi_{\text{Gd-Rad}} = \frac{4Ng^2\beta^2}{kT} \times \frac{7 + 15 \exp(4J_{\text{Gd-Rad}} / kT)}{7 + 9 \exp(4J_{\text{Gd-Rad}} / kT)} \quad (1)$$

$$\chi_M = \frac{\chi_{\text{Gd-Rad}}}{1 - (2zj' / Ng^2\beta^2)\chi_{\text{Gd-Rad}}} \quad (2)$$

The observed  $\chi_M T$  data were well reproduced (Fig. 6) by using the approximate eqn. (1-2), giving the best fitting parameters of  $g = 2.02$ ,  $J_{\text{Rad-Gd}} = 1.48 \text{ cm}^{-1}$ ,  $zj' = -0.014 \text{ cm}^{-1}$ . The positive value of  $J_{\text{Rad-Gd}}$  indicates the ferromagnetic interactions between Gd(III) and the radical, which is very common in the similar Gd(III)-radical complexes.<sup>19</sup> In addition, the negative  $zj'$  value indicates a very weak intermolecular antiferromagnetic interactions at low temperature.

The temperature dependence of magnetic susceptibility recorded for **5** and **6** revealed very similar behaviors (Fig. 6). At room temperature, the values of  $\chi_M T$  are 11.97 and 14.02  $\text{cm}^3 \cdot \text{K} \cdot \text{mol}^{-1}$  for **5** and **6** mononuclear complexes, respectively. Both of the values are very close to the expected values of 12.12 and 14.54  $\text{cm}^3 \cdot \text{K} \cdot \text{mol}^{-1}$  for an uncoupled system of one Ln(III) ion (Tb(III) or Dy(III)) and one radical. When the temperature is lowered, the  $\chi_M T$  values for **5** and **6** decrease slightly and reach values of 11.59 and 13.36  $\text{cm}^3 \cdot \text{K} \cdot \text{mol}^{-1}$  at about 40 K, respectively. Below this temperature, the  $\chi_M T$  values increase slowly to the highest value of 12.21  $\text{cm}^3 \cdot \text{K} \cdot \text{mol}^{-1}$  at 6 K (for **5**) and 13.62  $\text{cm}^3 \cdot \text{K} \cdot \text{mol}^{-1}$  at 7 K (for **6**), and then decreases on further cooling. The decrease of  $\chi_M T$  value upon lowering of the temperature in the high-temperature range for **5** and **6** is most probably governed by depopulation of the Ln<sup>III</sup> Stark sublevels. The increase of  $\chi_M T$  at low temperature suggests the presence of weak ferromagnetic interaction between the Tb(III) or Dy(III) ion and the coordinated NO group of organic radical.

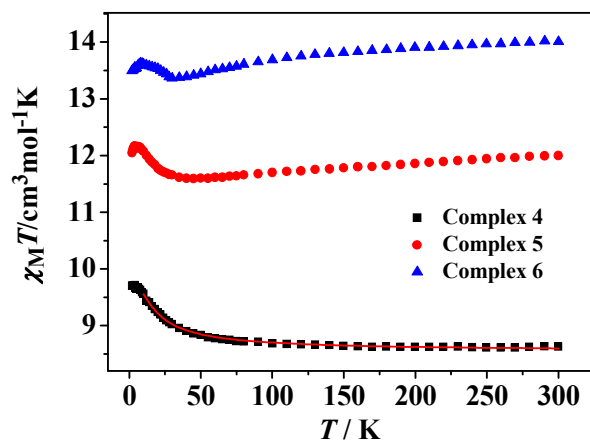


**Fig. 6.** Temperature dependence of  $\chi_M T$  values for complexes 4-6. The solid line represents the theoretical values based on the corresponding equations.

**Dynamic Magnetic Properties for Tb<sup>III</sup> and Dy<sup>III</sup>'s complexes (2, 3, 5, 6).** Tb<sup>III</sup> and Dy<sup>III</sup>'s complexes always have the tendency to be SMMs; therefore we performed the dynamic magnetic susceptibility measurements of complexes 2, 3, 5, 6.

For complex 2, no out-of-phase signals were observed above 2 K as shown in Fig. S5 (see ESI†). The temperature and frequency dependency data of the alternating current susceptibilities for 3 under zero dc field (Fig. 7) show strong frequency and temperature dependencies. From the temperature dependencies of the ac susceptibilities (Fig. 7, left), the in-phase ( $\chi'$ ) signals show a maximum at frequencies above 1000 Hz, and the out-of-phase ( $\chi''$ ) signals exhibit no maximum. From frequency dependencies of the ac susceptibility (Fig. 7, right), the magnetization relaxation times ( $\tau$ ) have been estimated between 2 and 2.5 K (Fig. 8a). Between 2.2~2.4 K, the relaxation follows a thermally activated mechanism affording an energy barrier of 6 K with a pre-exponential ( $\tau_0$ ) of  $4 \times 10^{-6}$  s based on Arrhenius law [ $\tau = \tau_0 \exp(U_{\text{eff}}/k_B T)$ ], which is consistent with those reported for similar SMMs (in the  $10^{-6}$ ~ $10^{-11}$  s range).<sup>27-28</sup> While at low temperatures a gradual crossover to a temperature-independent regime is observed. Below about 2.1 K, a dominant temperature-independent quantum regime of dynamics with a  $\tau$  value of 0.00025 s explains the absence of the  $M$  versus  $H$  hysteresis effect at 2 K (Fig. 5b). This may due to the hyperfine couplings and dipolar spin-spin interactions in lanthanide ions,

which allows fast quantum tunneling of magnetization that prevents the isolation of zero-field lanthanide SMMs with large barriers.<sup>5b,28b,29</sup> From frequency dependencies of the ac susceptibility measurements, Cole-Cole diagrams in the form of  $\chi''$  versus  $\chi'$  with nearly semicircular shapes have also been obtained (Fig. 8b). These data have been fitted to the generalized Debye model,<sup>30</sup> giving the small distribution coefficient  $\alpha$  value 0.13–0.09 (between 2~2.5 K), indicating the narrow distribution of relaxation times at these temperatures. The frequency shift parameter  $\varphi$  is 0.16 ( $\varphi = (\Delta T_p/T_p)/\Delta(\log \nu)$ ), excluding the possibility of spin-glass behavior.

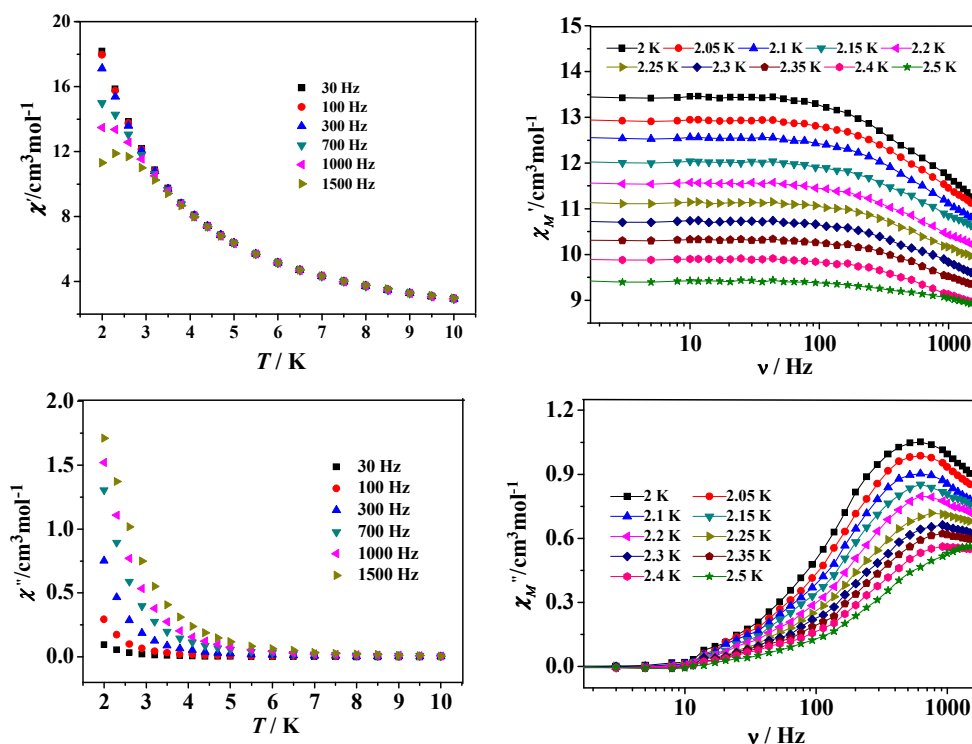


**Fig. 7.** Temperature dependence of the in-phase (top) and out-of-phase (bottom) components of the AC magnetic susceptibility for complex **3** under zero DC field at different frequencies (left). Frequency dependence of in-phase and out-of-phase susceptibilities under zero dc field at different temperatures for complex **3** (right).

For complex **5**, frequency-dependent out-of-phase signals are observed (Fig. 9), indicating the onset of magnetization expected for single-molecule magnet (SMM) behavior. However, no peak maximum is found above 2 K even for the highest

frequency investigated. This may result from quantum tunneling of the magnetization (QTM) that is too fast to be observed at the operating limits of our susceptometer. The imaginary component  $\chi''$  of the complex **6** does not show any frequency-dependent phenomenon (Fig. S6, see ESI<sup>†</sup>).

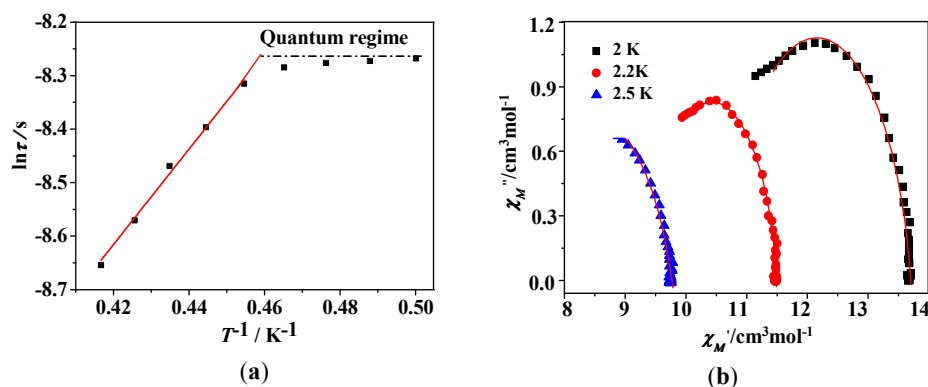


**Fig. 8.** (a) Magnetization relaxation time,  $\ln \tau$  vs  $T^{-1}$  plot for **3** under zero-dc field. The solid line is fitted with the Arrhenius law. (b) Cole–Cole plots measured at 2~2.5 K under zero dc field for complex **3**; the solid lines are the best fit to the experimental data.

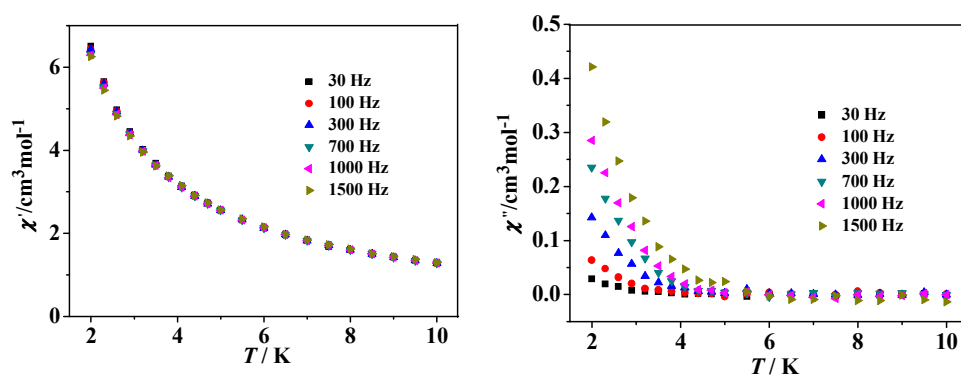


**Fig. 9.** Temperature dependence of the in-phase ( $\chi'$ ) and out-of-phase ( $\chi''$ ) components of the AC magnetic susceptibility for complex **5** under zero DC field.

As we seen, by using Phtfac to replace hfac as  $\beta$ -diketonate, the crystal structures of complexes **5** and **6** show drastic changes compared with **2** and **3**. In **2** and **3**, two  $\text{Ln}(\text{hfac})_3$  units are connected by a radical ligand MeTrzNIT to give binuclear cores, and the center  $\text{Ln}^{\text{III}}$  ions are all surrounded with a slightly distorted 4,4,4-tricapped trigonal

prism LnO<sub>8</sub>N coordination sphere. In **5** and **6**, the central Ln<sup>III</sup> ions exhibit mononuclear structure, which are in an LnO<sub>7</sub>N coordination sphere with *D*<sub>4d</sub> symmetry. In addition, the presence of the different magnetic exchange coupling between the radical and metal ion in the two Tb's complexes or the two Dy's complexes will moderate their magnetic relaxation behaviors. It has been demonstrated that the ferromagnetic coupling between radical and 4f ions could enhance the anisotropy.<sup>22,31</sup> Owing to the differences in crystal structure and magnetic interaction between the spin carriers, there is also obvious change in their magnetic behavior: complex **2** shows no obvious magnetic relaxation whereas complex **5** exhibits SMM behavior. Complex **3** affords a barrier of 6 K while complex **6** has no visible magnetic relaxation. These results suggest that the local ligand-field of the Ln(III) ions and the magnetic coupling between the radical and Ln(III) ion are responsible for the different magnetic dynamic behaviors. It is evident that replacement of the CF<sub>3</sub> group by a phenyl ring results in a significant change in magnetic relaxation and this provides an opportunity to fine-tune Ln-radical based SMM behavior through the modification of the β-diketonate coligand of lanthanide ion.

## Conclusions

In summary, six novel binuclear or mono lanthanide-radical compounds have been synthesized using a triazole nitronyl nitroxide radical ligand and two different β-diketonate coligands. By using hexafluoroacetylacetone (hfac) as coligand, three binuclear tri-spin complexes were obtained, in which the nitronyl nitroxide moiety acts as a double-bridge ligand linking two Ln(III) ions by the two oxygen atoms of the N-O groups and the two nitrogen atoms of the triazole ring. When hfac were replaced by 4,4,4-trifluoro-1-phenylbutane-1,3-dione (Phtfac), three isomorphous mononuclear complexes **4-6** were obtained. The study of dynamics of the magnetizations for complexes **2, 3, 5, 6** shows that they exhibit quite distinct magnetic relaxation behaviors. Complex **3** and **5** shows frequency-dependent out-of-phase signals, however, such a phenomena is not observed for **2** and **6**. The difference in magnetic relaxation of these complexes is probably due to the different symmetry of local ligand field of the Ln(III)

(Tb and Dy) ions together with the different magnetic exchange coupling. These results show that the different ligand field can drastically affect the magnetic relaxation of the magnetization. Theoretical studies are required thoroughly analyze the symmetry of local ligand field of the Ln(III) ion/dynamic of the magnetization relationship.

## Acknowledgements

This work was financially supported by the National Natural Science Foundation of China (21371133).

## Appendix A. Supplementary material

CCDC 1057820, 1057821, 1057822 and 1431964 contain the supplementary crystallographic data for **1-4**. These data can be obtained free of charge via [www.ccdc.cam.ac.uk/conts/retrieving.html](http://www.ccdc.cam.ac.uk/conts/retrieving.html) (or from the Cambridge Crystallographic Centre, 12 Union Road, Cambridge CB21EZ, UK; Fax: (+44) 1223-336033; or [deposit@ccdc.cam.ac.uk](mailto:deposit@ccdc.cam.ac.uk)).

## References

- 1 (a) R. Sessoli, D. Gatteschi and M. A. Novak, *Nature*, 1993, **365**, 141; (b) G. Christou, D. Gatteschi, D. N. Hendrickson and R. Sessoli, *MRS Bull.*, 2000, 25, 66;
- 2 (a) A. Caneschi, D. Gatteschi, N. Laloti, C. Sangregorio, R. Sessoli, G. Venturi, A. Vindigni, A. Rettori, M. G. Pini and M. A. Novak, *Angew. Chem., Int. Ed.*, 2001, **40**, 1760; (b) R. Clérac, H. Miyasaka, M. Yamashita and C. Coulon, *J. Am. Chem. Soc.*, 2002, **124**, 12837; (c) C. Coulon, H. Miyasaka and R. Clérac, *Struct. Bonding*, 2006, **122**, 163; (d) D. Gatteschi, R. Sessoli and J. Villain, *Molecular Nanomagnets*, Oxford University Press, Oxford, 2006; (e) L. Bogani, A. Vindigni, R. Sessoli and D. Gatteschi, *J. Mater. Chem.*, 2008, **18**, 4750.
- 3 (a) L. Thomas, F. Lioni, R. Ballou, D. Gatteschi, R. Sessoli and B. Barbara, *Nature*, 1996, **383**, 145; (b) J. R. Friedman, M. P. Sarachik, J. Tejada and R. Ziolo, *Phys. Rev. Lett.*, 1996, **76**, 3830; (c) J. A. Jones, *Science* 1998, **280**, 229; (e) W. Wernsdorfer, N. Aliaga-Alcalde, D. N. Hendrickson and G. Christou, *Nature*, 2002, **416**, 406; (d) B. Barbara, *Inorg. Chim. Acta*, 2008, **361**, 3371.
- 4 (a) M. N. Leuenberger and D. Loss, *Nature*, 2001, **410**, 789; (b) L. Bogani and W. Wernsdorfer, *Nat. Mater.*, 2008, **7**, 179; (c) M. Mannini, F. Pineider, C. Danieli, F.

- Totti, L. Sorace, Ph. Saintavit, M. A. Arrio, E. Otero, L. Joly, J. C. Cezar, A. Cornia and R. Sessoli, *Nature*, 2010, **468**, 417.
- 5 (a) P. D. W. Boyd, Q. Li, J. B. Vincent, K. Folting, H. R. Chang, W. E. Streib, J. C. Huffman, G. Christou and D. N. Hendrickson, *J. Am. Chem. Soc.*, 1988, **110**, 8537; (b) N. Ishikawa, M. Sugita and W. Wernsdorfer, *Angew. Chem.* 2005, **117**, 2991; *Angew. Chem. Int. Ed.* 2005, **44**, 2931; (c) X. Y. Wang, Z. M. Wang, S. Gao, *Chem. Commun.*, 2008, **44**, 281.
- 6 D. Gatteschi and R. Sessoli, *Angew. Chem., Int. Ed.*, 2003, **42**, 269.
- 7 (a) A. Caneschi, D. Gatteschi, N. Lalioti, C. Sangregorio, R. Sessoli, G. Venturi, A. Vindigni, A. Rettori, M. G. Pini and M. A. Novak, *Angew. Chem.*, 2001, **113**, 1810; (b) H. L. Sun, Z. M. Wang and S. Gao, *Coord. Chem. Rev.*, 2010, **254**, 1081; (c) J. S. Miller and D. Gatteschi, *Chem. Soc. Rev.*, 2011, **40**, 3065.
- 8 (a) J. K. Tang, I. Hewitt, N. T. Madhu, G. Chastanet, W. Wernsdorfer, C. E. Anson, C. Benelli, R. Sessoli and A. K. Powell, *Angew. Chem., Int. Ed.*, 2006, **45**, 1729; (b) K. Bernot, J. Luzon, L. Bogani, M. Etienne, C. Sangregorio, M. Shanmugam, A. Caneschi, R. Sessoli and D. Gatteschi, *J. Am. Chem. Soc.*, 2009, **131**, 5573; (c) K. Bernot, F. Pointillart, P. Rosa, M. Etienne, R. Sessoli and D. Gatteschia, *Chem. Commun.*, 2010, **46**, 6458.
- 9 (a) P. H. Lin, T. J. Burchell, R. Clérac and M. Murugesu, *Angew. Chem., Int. Ed.*, 2008, **47**, 8848; (b) G. F. Xu, Q. L. Wang, P. Gamez, Y. Ma, R. Clérac, J. K. Tang, S. P. Yan, P. Cheng and D. Z. Liao, *Chem. Commun.*, 2010, **46**, 1506; (c) R. A. Layfield, J. J. W. McDouall, S. A. Sulway, F. Tuna, D. Collison and R. E. P. Winpenny, *Chem.–Eur. J.*, 2010, **16**, 4442.
- 10 (a) I. J. Hewitt, Y. Lan, C. E. Anson, J. Luzon, R. Sessoli and A. K. Powell, *Chem. Commun.*, 2009, **45**, 6765; (b) K. Isele, F. Gigon, A. F. Williams, G. Bernardinelli, P. Franz and S. Decurtins, *Dalton Trans.*, 2007, 332; (c) K. W. Galloway, A. M. Whyte, W. Wernsdorfer, J. Sanchez-Benitez, K. V. Kamenev, A. Parkin, R. D. Peacock and M. Murrie, *Inorg. Chem.*, 2008, **47**, 7438; (d) P. H. Lin, T. J. Burchell, L. Ungur, L. F. Chibotaru, W. Wernsdorfer and M. Murugesu, *Angew. Chem., Int. Ed.*, 2009, **48**, 9489; (e) Y. N. Guo, G. F. Xu, P. Gamez, L. Zhao, S. Y. Lin, R. P. Deng, J. K. Tang and H. J. Zhang, *J. Am. Chem. Soc.*, 2010, **132**, 8538.
- 11 J. D. Rinehart, M. Fang, W. J. Evans and J. R. Long, *Nat. Chem.*, 2011, **3**, 538.
- 12 Y. N. Guo, G. F. Xu, W. Wernsdorfer, L. Ungur, Y. Guo, J. Tang, H. J. Zhang, L. F. Chibotaru and A. K. Powell, *J. Am. Chem. Soc.*, 2011, **133**, 11948.
- 13 A. Caneschi, D. Gatteschi, N. Lalioti, C. Sangregorio, R. Sessoli, G. Venturi, A. Vindigni, A. Rettori, M. G. Pini and M. A. Novak, *Angew. Chem., Int. Ed.*, 2001, **40**, 1760.
- 14 (a) N. Ishii, Y. Okamura, S. Chiba, T. Nogami and T. Ishida, *J. Am. Chem. Soc.*, 2008, **130**, 24; (b) C. Benelli and D. Gatteschi, *Chem. Rev.*, 2002, **102**, 2369; (c) D. Luneau and P. Rey, *Coord. Chem. Rev.*, 2005, **249**, 2591; (c) R. N. Liu, L. C. Li, X. L. Wang, P. P. Yang, C. Wang, D. Z. Liao and J. P. Sutter, *Chem. Commun.*, 2010, **46**, 2566.
- 15 (a) K. Fegy, D. Luneau, T. Ohm, C. Paulsen, P. Rey, *Angew. Chem.*, 1998, **110**, 1331; *Angew. Chem. Int. Ed.*, 1998, **37**, 1270; (b) Y. Z. Zheng, Y. Lan, C. E. Anson,

- A. K. Powell, *Inorg. Chem.*, 2008, **47**, 10813; (c) S. Kanegawa, M. Maeyama, M. Nakano, N. Koga, *J. Am. Chem. Soc.*, 2008, **130**, 3079; (d) S. Katagiri, Y. Tsukahara, Y. Hasegawa, Y. Wada, *Bull. Chem. Soc. Jpn.*, 2007, **80**, 1492.
- 16 A. Lang, Y. Pei, L. Ouahab, O. Kahn, *Adv. Mater.*, 1996, **8**, 60.
- 17 (a) G. M. Sheldrick, SHELXS-97, *Program for Solution of Crystal Structures*, University of Göttingen, Germany, 1997; (b) G. M. Sheldrick, SHELXL-97, *Program for Refinement of Crystal Structures*, University of Göttingen, Germany, 1997; (c) G. M. Sheldrick, SADABS, *Program for Area Detector Adsorption Correction*, Institute for Inorganic Chemistry, University of Göttingen, Germany, 1996.
- 18 C. J. O'Connor, *Prog. Inorg. Chem.*, 1982, **29**, 203.
- 19 (a) C. Benelli, A. Caneschi, D. Gatteschi, L. Pardi, P. Rey, D. P. Shum and R. L. Carlin, *Inorg. Chem.*, 1989, **28**, 272; (b) J. P. Sutter, M. L. Kahn, S. Golhen, L. Ouahab and O. Kahn, *Chem. Eur. J.* 1998, **4**, 571; (c) Y. L. Wang, Y. Y. Gao, Y. Ma, Q. L. Wang, L. C. Li and D. Z. Liao, *CrystEngComm*, 2012, **14**, 4706; (d) C. Benelli, A. Caneschi, D. Gatteschi, J. Laugier and P. Rey, *Angew. Chem., Int. Ed.*, 1987, **26**, 913; (e) C. Lescop, G. Bussiere, R. Beaulac, H. Beslisle, E. Beloeizky, P. Rey, C. Reber and D. Luneau, *J. Phys. Chem. Solids*, 2004, **65**, 773; (f) N. Zhou, Y. Ma, C. Wang, G. F. Xu, J. K. Tang and D. Z. Liao, *J. Solid State Chem.*, 2010, **183**, 927; (g) Q. H. Zhao, Y. P. Ma, L. Du and R. B. Fang, *Transition Met. Chem.*, 2006, **31**, 593.
- 20 Y. Q. Sun, L. L. Fan, D. Z. Gao, Q. L. Wang, M. Du, D. Z. Liao and C. X. Zhang, *Dalton Trans.*, 2010, **39**, 9654.
- 21 S. Y. Zhou, X. Li, T. Li, L. Tian, Z. Y. Liu and X. G. Wang, *RSC Adv.*, 2015, **5**, 17131.
- 22 C. Aronica, G. Pilet, G. Chastanet, W. Wernsdorfer, J. F. Jacquot, D. Luneau, *Angew. Chem., Int. Ed.* 2006, **45**, 4659.
- 23 (a) J. X. Xu, Y. Ma, D. Z. Liao, G. F. Xu, J. K. Tang, C. Wang, N. Zhou, S. P. Yan, P. Cheng and L. C. Li, *Inorg. Chem.*, 2009, **48**, 8890; (b) P. Hu, X. F. Wang, Y. Ma, Q. L. Wang, L. C. Li and D. Z. Liao, *Dalton Trans.*, 2014, **43**, 2234.
- 24 (a) S. Osa, T. Kido, N. Matsumoto, N. Re, A. Pochaba and J. Mrozinski, *J. Am. Chem. Soc.*, 2004, **126**, 420; (b) K. Bernot, L. Bogani, R. Sessoli and D. Gatteschi, *Inorg. Chim. Acta*, 2007, **360**, 3807; (c) Y. Ma, G. F. Xu, X. Yang, L. C. Li, J. K. Tang, S. P. Yan, P. Cheng and D. Z. Liao, *Chem. Commun.*, 2010, **46**, 8264; (d) Y. M. Bing, N. Xu, W. Shi, K. Liu and P. Cheng, *Chem.-Asian J.*, 2013, **8**, 1412.
- 25 (a) X. L. Mei, Y. Ma, L. C. Li and D. Z. Liao, *Dalton Trans.*, 2012, **41**, 505; (b) X. L. Mei, R. N. Liu, C. Wang, P. P. Yang, L. C. Li and D. Z. Liao, *Dalton Trans.*, 2012, **41**, 2904.
- 26 (a) N. Zhou, Y. Ma, C. Wang, G. F. Xu, J. K. Tang, J. X. Xu, S. P. Yan, P. Cheng, L. C. Li and D. Z. Liao, *Dalton Trans.*, 2009, **38**, 8489; (b) T. Han, W. Shi, X. P. Zhang, L. L. Li and P. Cheng, *Inorg. Chem.*, 2012, **51**, 13009.
- 27 (a) S. D. Jiang, B. W. Wang, G. Su, Z. M. Wang and S. Gao, *Angew. Chem., Int. Ed.* 2010, **49**, 7448; (b) G. J. Chen, C. Y. Gao, J. L. Tian, J. K. Tang, W. Gu, X. Liu, S. P. Yan, D. Z. Liao and P. Cheng, *Dalton Trans.*, 2011, **40**, 5579; (c) G. J. Chen, Y. N.

- Guo, J. L. Tian, J. K. Tang, W. Gu, X. Liu, S. P. Yan, P. Cheng and D. Z. Liao, *Chem. Eur. J.*, 2012, **18**, 2484; (d) Y. L. Wang, Y. Ma, X. Yang, J. K. Tang, P. Cheng, Q. L. Wang, L. C. Li and D. Z. Liao, *Inorg. Chem.* 2013, **52**, 7380; (e) H. X. Tian, R. N. Liu, X. L. Wang, P. P. Yang, Z. X. Li, L. C. Li and D. Z. Liao, *Eur. J. Inorg. Chem.*, 2009, 4498; (f) R. N. Liu, C. M. Zhang, L. C. Li, D. Z. Liao and J.-P. Sutter, *Dalton Trans.*, 2012, **41**, 12139; (g) F. Pointillart, K. Bernot, G. Poneti, and Roberta Sessoli, *Inorg. Chem.*, 2012, **51**, 12218.
- 28 (a) Y. Wang, X. L. Li, T. W. Wang, Y. Song and X. Z. You, *Inorg. Chem.*, 2010, **49**, 969; (b) D. P. Li, T. W. Wang, C. H. Li, D. S. Liu, Y. Z. Li and X. Z. You, *Chem. Commun.*, 2010, **46**, 2929; (c) J. Liu, X. P. Zhang, T. Wu, B. B. Ma, T. W. Wang, C. H. Li, Y. Z. Li and X. Z. You, *Inorg. Chem.*, 2012, **51**, 8649.
- 29 (a) F. Luis, M. Martínez-Pérez,; O. Montero, E. Coronado, S. Cardona-Serra, C. Martí-Gastaldo, J. M. Clemente-Juan, J. Sesé, D. Drung and T. Schurig, *Phys. Rev. B*, 2010, **82**, 060403; (b) R. Giraud, W. Wernsdorfer, A. M. Tkachuk, D. Mailly and B. Barbara, *Phys. Rev. Lett.*, 2001, **87**, 057203.
- 30 (a) K. S. Cole and R. H. Cole, *J. Chem. Phys.*, 1941, **9**, 341; (b) S. M. J. Aubin, Z. Sun, L. Pardi, J. Krzystek, K. Folting, L. C. Brunel, A. L. Rheingold, G. Christou and D. N. Hendrickson, *Inorg. Chem.*, 1999, **38**, 5329.
- 31 J. Long, F. Habib, P.-H. Lin, I. Korobkov, G. Enright, L. Ungur, W. Wernsdorfer, L. F. Chibotaru and M. Murugesu, *J. Am. Chem. Soc.*, 2011, **133**, 5319.

Title: Modulating spin dynamics of Ln<sup>III</sup>-radical complexes by using  
different coligand

Authors: Ting Li, Shang Yong Zhou, Xin Li, Li Tian\*, Dai Zheng Liao, Zhong Yi Liu  
and Jian Hua Guo

**Contents graphic and synopsis**

Six Ln<sup>III</sup>-triazole-radical complexes have been synthesized by using different  $\beta$ -diketonate coligand, they exhibit interesting magnetic properties. Complex **3** and **5** shows frequency-dependent ac magnetic susceptibilities, which suggests the presence of slow magnetic relaxation. It is evident that the  $\beta$ -diketonate coligand play an important role in determining the spin dynamic for the lanthanide-radical system.

